Published in final edited form as:
Cell Metab. 2014 May 6; 19(5): 836–848. doi:10.1016/j.cmet.2014.03.023.

PTENα is a PTEN isoform Translated through Alternative Initiation and Regulates Mitochondrial Function

Hui Liang[1,3], **Shiming He**[1,3], **Jingyi Yang**[1], **Xinying Jia**[1,2], **Pan Wang**[1], **Xi Chen**[1], **Zhong Zhang**[1,2], **Xiajuan Zou**[1], **Michael A. McNutt**[1], **Wen Hong Shen**[2,*], and **Yuxin Yin**[1,*]

[1]Institute of Systems Biomedicine, Department of Pathology, School of Basic Medical Sciences, Center for Age-related Diseases, Peking University Health Science Center, Beijing, 100191, P. R. China

[2]Department of Radiation Oncology, Weill Medical College of Cornell University, New York, NY 10065, USA

Summary

PTEN is one of the most frequently mutated genes in human cancer. It is known that PTEN has a wide range of biological functions beyond tumor suppression. Here we report that PTENα, an N-terminally extended form of PTEN, functions in metabolism. Translation of PTENα is initiated from a CUG codon upstream of and in-frame with the coding region of canonical PTEN. Eukaryotic translation initiation factor 2A (eIF2A) controls PTENα translation and a CUG-centered palindromic motif is required in this process. PTENα induces cytochrome c oxidase activity and ATP production in mitochondria. TALEN-mediated somatic deletion of PTENα impairs mitochondrial respiratory chain function. We show that PTENα interacts with canonical PTEN to increase PINK1 and promote energy production. These data provide insights into the mechanism by which the PTEN family is involved in multiple cellular processes. Our studies suggest that mammalian cells can use alternate translation initiation mechanisms to generate protein isoforms.

Introduction

PTEN is one of the most frequently mutated genes in human cancer (Li et al., 1997; Steck et al., 1997; Teng et al., 1997). Germline mutations of *PTEN* are associated with tumorsusceptibility diseases, such as Cowden syndrome, which is characterized by multiple hamartomas (Liaw et al., 1997; Nelen et al., 1997). The role of PTEN as a potent tumor

[*]Correspondence to: Yuxin Yin, M.D., Ph.D., University Professor and Director, Institute of Systems Biomedicine, Dean, School of Basic Medical Sciences, Peking University Health Science Center, Beijing 100191, P.R China, Phone (86) 10-8280-1237, Fax: (86) 10-8280-1380, yinyuxin@hsc.pku.edu.cn; Wen Hong Shen, Ph.D., Assistant Professor, Department of Radiation Oncology, Weill Cornell Medical College, 515 E. 71st Street, S127, New York, NY 10021, Phone (212) 746-1314, Fax: (212) 746-0095, wes2007@med.cornell.edu.
[3]These authors contributed equally to this work

suppressor has been demonstrated in many animal models, where *Pten* deletion leads to development of various types of tumors that mimic the spectrum of human cancers associated with *PTEN* mutations (Di Cristofano et al., 1998; Podsypanina et al., 1999; Stambolic et al., 2000). *Pten* loss also results in neurological defects and metabolic disorders (Gasser, 2007; Stiles et al., 2004; Stiles et al., 2006), suggesting that PTEN function is not limited to tumor suppression. PTEN is essential for embryonic development as homozygous *Pten* deletion results in developmental defects and embryonic lethality (Di Cristofano et al., 1998; Podsypanina et al., 1999; Suzuki et al., 1998). These findings all demonstrate the importance of PTEN in a diversity of biological processes including embryonic development, tissue homeostasis, metabolism, and tumor suppression.

PTEN resides at the 10q23 locus and encodes a 403-amino-acid protein with an N-terminal phosphatase domain (Li et al., 1997; Steck et al., 1997). The primary substrate of PTEN phosphatase is phosphatidylinositol-3,4,5-triphosphate (PIP3), a critical messenger for activation of the phosphoinositide-3-kinase (PI3K)/AKT pathway (Maehama and Dixon, 1998). PTEN dephosphorylates PIP3 at the plasma membrane, and negatively regulates PI3K/AKT-mediated cell survival and proliferation. In the nucleus, PTEN maintains chromosomal integrity by stabilizing centromeres (Shen et al., 2007) and regulates cellular senescence through APC-CDH1-mediated protein degradation (Song et al., 2011). These nuclear PTEN functions are phosphatase-independent and unrelated to the PI3K/AKT pathway (Shen et al., 2007; Song et al., 2011). These findings indicate that PTEN functions to control diverse fundamental biological processes, which cannot be attributed merely to its phosphatase activity or to its regulation of the PI3K/AKT pathway. It is therefore likely that some severe observed consequences of PTEN dysfunction result from loss of PTEN functions that are as yet unidentified. Alternatively, unidentified forms of PTEN may exist that serve in roles previously assumed to be functions of canonical PTEN.

PTEN is an evolutionarily conserved protein and has been considered to be genetically unique without other isoforms. In this study, we identified an alternate translation initiation at a CUG site in the 5′-untranslated region (5′-UTR) of PTEN mRNA. This CUG start codon generates a larger form of PTEN with an elongated N-terminal region comprising an additional 173 (*Homo sapiens*) or 169 (*Mus musculus*) amino acids. We used multiple approaches to demonstrate the existence of this new form of PTEN, which we have designated PTENα. We show that eIF2A-dependent CUG initiation is involved in PTENα synthesis and a CUG-centered palindromic sequence is required for this process. PTENα is involved in the eukaryotic electron transport process through induction of cytochrome c oxidase activity in mitochondria, and disruption of PTENα impairs mitochondrial bioenergetics. These results establish that a PTEN isoform of greater length and additional functions is produced by an alternative CUG translation initiation. Identification of PTENα suggests re-interpretation of the importance of PTEN in multiple fundamental cellular activities is warranted.

Results

An unknown 70 kDa Protein Shares an Expression Pattern with PTEN and is Recognized by PTEN Antibodies

We have been interested in gene regulation in response to cellular stresses, particularly oxidative stress (Liu et al., 2008; Shen et al., 2006; Yin et al., 2003). During study of PTEN response to oxidative stress, we found PTEN expression is reduced following H_2O_2 treatment. We also noticed that a full-length PTEN antibody reacted with an unidentified protein of higher molecular weight (around 70 kDa, Figure S1A) and this protein is expressed in a pattern identical to PTEN. To determine whether differences in PTEN status may affect this larger PTEN-like protein, we examined a panel of cancer cell lines and found that this 70-kDa protein is undetectable in PTEN-null cells (Figure S1B). A rabbit monoclonal PTEN antibody against the PTEN C-terminal domain also recognizes this PTEN-like protein (Figure S1B), indicating it likely shares a C-terminal region with regular PTEN. These observations suggest a longer form of PTEN with the same C-terminal region may exist. We designate this PTEN-like protein as PTENα.

PTENα Translationally Initiated from CUG^{513}

Leucine-initiator tRNA-mediated translation starts at CUG codons is a recently discovered mechanism of translation initiation (Starck et al., 2012). We evaluated the 5′-UTR of PTEN mRNA for alternative translation start sites and found a total of six alternative CUG initiation codons in-frame with the canonical AUG^{1032} start codon. Translation initiation from the first two CUGs (highlighted in Figure 1A), CUG^{513} or CUG^{639}, would encode larger forms of PTEN comprising 576 or 534 amino acids respectively with predicted molecular weights of 61-65 kDa. A protein of this size may be expected to migrate at ∼70 kDa via gel electrophoresis, which matches our observed PTENα band.

Closer assessment of these CUGs reveals a 16-bp perfect palindromic sequence centered on CUG^{513} (CCCGCUCCUGGAGCGGG, underlined in red, Figure 1A), which may represent a signature motif for translation initiation. Further phylogenetic analysis suggests that the PTENα start codon and the surrounding palindromic sequence are evolutionary conserved (Figure 1B). PTEN CTG^{513} is 173 amino acids upstream of the canonical methionine start codon ATG^{1032}. To determine whether this CUG can initiate translation of this putative PTENα protein with upstream extension of the open reading frame (ORF), we constructed a PTENα expression plasmid. As expected, the CTG^{513}-initiated PTENα ORF is translated into two distinct proteins with masses of 70 kDa (PTENα) and 55 kDa (canonical PTEN) (Figure 1C). It is of note that PTENα is expressed at lower abundance than PTEN. This expression pattern is reversed when translation of PTENα is initiated by the ATG start codon of N-terminal inserted FLAG tag, and the 70^{+}-kDa FLAG-PTENα band becomes dominant (Figure 1C). This reversal indicates that CUG^{513} is a weaker initiator codon than AUG^{1032}. These data suggest that PTENα can be translated from a new ORF beginning with CUG codon(s) in the 5′-UTR of PTEN mRNA upstream of the canonical AUG start codon.

To confirm CUG-initiated translation of PTENα, we constructed a set of plasmids for expression of ATG^{1032}-starting PTEN and CTG^{513}-starting PTENα, both with a C-terminal GFP tag (Figures 1D and 1E). As both CTG^{513} and CTG^{639} can initiate the translation of proteins of a similar size (~70 kDa), we created a mutation on each of these two CTGs separately to determine which is necessary for PTENα expression. While PTEN-GFP expression is not affected by mutation at either one of these two sites, GFP-PTENα is differentially altered. Mutation at CTG^{513} greatly diminishes PTENα, whereas mutation at CTG^{639} has no such effect (Figures 1F and 1G). These results indicate that CTG^{513}, but not CTG^{639}, is required for PTENα expression and that CTG^{513} is likely the translation initiation site for PTENα. These results are consistent with similar mutagenesis assays obtained from other expression systems (Figure S1C). The mutation of CTG^{513} but not CTG^{639} into GGA or CTA (coding the same amino acid, Leucine, as CTG) abolishes the PTENα band without decreasing expression of PTEN, while mutation of both sites elicits a similar specific elimination of PTENα (Figures S1D and S1E). Further mutagenesis analysis suggests that switching ATG and CTG can reverse the dominance hierarchy status of PTEN and PTENα. While mutation of ATG^{1032} to ATA eliminates canonical PTEN (Figure S1E), replacement of CTG^{513} with ATG and ATG^{1032} with GGA results in elevation of PTENα and reduction of PTEN (Figure S1D). These data collectively demonstrate that PTENα synthesis relies on an alternative translation initiation at the CUG^{513} codon.

Mass Spectrometry Analysis Reveals the PTENα Sequence

In order to validate the PTENα translation start site, we sought direct evidence using mass spectrometry for peptide sequencing. We first purified PTENα with a C-terminal His tag (Figure 2A) expressed in E. coli for mass spectrometry (Figure 2B). Mascot reports reveal six peptide fragments covering 55.5% of the N-terminal region of PTENα (from CTG^{513} to ATG^{1032}, designated as αN, Figure 2B). In particular, the most proximal N-terminal peptide (17-aa, MS/MS spectrum shown in Figure 2C) is mapped near the first leucine initiator (CTG^{513}), suggesting that CTG^{513} is the initiation site for PTENα translation.

Regular LC-MS/MS captures the 17-aa peptide adjacent to the PTENα N-terminus, but not the 3-aa proximal end, LER. To improve the chances of trapping this small fragment, we purified a C-terminally His-tagged PTENα protein expressed in Sf9 insect cells (Figures 2D and 2E) and utilized the TMPP-Ac-Osu derivatization approach (Chen et al., 2007; Huang et al., 1999) for MALDI-TOF/TOF MS and *de novo* sequencing. This resulted in the identification of the first three N-terminal amino acids of PTENα, LER (Figures 2F and 2G). The mass spectrum data confirm that CUG^{513} is the PTENα translation initiation site.

Validation of the PTENα Gene Locus and Translation Initiation Using a C-terminal FLAG-knock-in Mouse Model

Comparison of the 5′-UTR of *Homo sapiens PTEN* and *Mus musculus Pten* reveals 95% homology (Figure S2A), suggesting a similar alternative translational initiation mechanism may also apply in mice. In order to further identify the gene locus of *Pten*α and its translation initiation site, we generated a FLAG-knock-in mouse model ($Pten^{FLAG}$), in which the C-terminus of the *Pten* gene was targeted for insertion of a FLAG-coding sequence (Figures 2H and S2B). To verify the existence of *Pten*α at the *Pten* gene locus,

tissue samples were extracted from heterozygous *Pten*^{FLAG} mice and wild-type control mice for FLAG pull-down. Theoretically, a FLAG pull down procedure will reveal all potential *Pten* isoforms with the same FLAG-tagged C-terminus but varying lengths of N-termini. Two distinct protein bands are detectable in the FLAG elute from *Pten*^{FLAG} tissues, with molecular masses of 70- and 55-kDa (Figure S2C). No *Pten* is detected in wild-type tissues (Figures 2I and S2C). The two forms of FLAG-tagged Pten protein found in *Pten*^{FLAG} knock-in mice are of molecular masses similar to the two endogenous Pten forms previously observed in MEFs (Figure S2C). The 70-kDa band in MEFs was recognized by an antibody raised against the PTENα-specific N-terminal region (referred to as αN, Figures S2D and S2E). The existence of *in vivo* Ptenα with an N-terminally extended αN region was further confirmed by mass spectrometric analysis of a FLAG-purified 70^{+}-kDa band from *Pten*^{FLAG} tissues (Figure 2J). One of the six identified Ptenα peptides (167-175: LPDmTAIIK, underlined) spans the border of αN and PTEN. The evidence *that Pten*^{FLAG} knock-in tissues express C-terminal FLAG-tagged Ptenα suggests that Ptenα and Pten can be translated *in vivo* from the same mRNA at the same gene locus. The *Pten*^{FLAG} knock-in animal model demonstrates the natural occurrence of alternative initiation that results in the translation of Ptenα.

Critical Role of eIF2A-mediated CUG Initiation in PTENα Synthesis

The eIF2A-dependent mechanism plays an important role in initiation at CUG start codons with leucine and structurally distinct compounds can differentially inhibit protein synthesis initiated by AUG or CUG start codons. For example, acriflavine inhibits CUG initiation whereas aurin trycarboxylic acid (ATA) inhibits initiation at the AUG start codon but enhances CUG initiation (Starck et al., 2012). We examined expression levels of PTENα in response to these chemical inhibitors and found that ATA, a known enhancer of CUG initiation, induces PTENα expression (Figures 3A). On the other hand, acriflavine reduces PTENα expression in a dose-dependent manner without affecting PTEN expression (Figures 3B). Overexpression of eIF2A significantly increases PTENα expression (Figure 3C), whereas PTENα is downregulated in eIF2A knockdown cells (Figure 3D). These data indicate that PTENα is synthesized through an eIF2A-mediated translation CUG initiation mechanism.

As noted earlier, CUG^{513} is embedded in a 16-bp palindromic motif (Figure 1A, underlined sequence). Many previously reported genes with the CUG start codon have similar CUG-centered palindromic sequences (Figure S3A). In order to determine whether this motif influences translation initiation at CUG^{513}, we constructed PTENα mutants to disrupt the palindrome (Figure 3E) and examined PTENα expression. Mutation of the nucleotide triplets immediately upstream or downstream of CUG^{513} (CTC^{510}>TAG or TAT, or CAG^{516}>TCT) greatly reduces PTENα expression (Figures 3F and S3B). At the same time, disruption of this palindromic motif by direct mutation of CUG^{513} itself to either CUA or AAA leads to a greater reduction of PTENα (Figure 3F). Interestingly, the alteration CTC^{510}>TAT at the 5′ end of the CUG start codon leads to about 50% decrease in levels of PTENα, while GAG^{516}>TCT, which lies exactly on the opposite side of the palindrome decreases PTENα to a mere 5-10%, implying that the positions at the 3′ end are more important than those at the 5′ end. These data suggest that the palindromic sequence

surrounding CUG^{513} may serve as a signal for CUG initiation site recognition, in a manner similar to the Kozak sequence for AUG initiation.

Localization of PTENα in Mitochondria

To examine the subcellular localization of PTENα and compare it with that of PTEN, we first employed a protease protection assay. Cells transfected with N-terminal or C-terminal GFP-tagged PTENα or PTEN were subjected to consecutive digestion with digitonin (cytoplasmic membrane permeabilization) and trypsin (removal of cytosolic exposed terminus of organelle-associated protein). To make sure only one isoform is expressed, we created an ATG^{1032}>ATA mutation in GFP-tagged PTENα. As shown in Figure 4A, PTENα exhibits a distinct signal pattern as compared with PTEN, with and without protease digestion. Prior to digitonin treatment, PTEN is ubiquitously distributed in both the cytoplasm and the nucleus, but PTENα displays predominantly cytoplasmic localization. Digitonin treatment eliminates the majority of the cytoplasmic PTEN signal but partially retains PTENα signals, suggesting that PTENα can be cytosolic or associated with cytoplasmic organelles whereas PTEN is mainly cytosolic. Further trypsin digestion removes all PTEN signals but does not affect digitonin-retained PTENα signals, regardless of the GFP position. It appears that PTENα is predominantly localized in the cytoplasm and may have multiple intracellular forms including a cytosolic form (protease sensitive) and an organelle-associated form (protease insensitive). We next used MitoTracker to label mitochondria and evaluate potential colocalization of C-terminal GFP-tagged PTENα or PTEN with mitochondria. We observed substantial colocalization of PTENα with mitochondria, whereas mitochondrial colocalization is less prominent for PTEN (Figure 4B). To determine whether endogenous PTENα can be detected in mitochondria, we performed a fractionation procedure to separate the mitochondria from the cytoplasm. PTENα is found in the mitochondrial fraction of *Pten*$^{+/+}$ MEFs, whereas canonical PTEN is found primarily in the cytoplasmic fraction (Figure 4C). Further evaluation of submitochondrial localization suggests that PTENα is preferentially associated with the mitochondrial inner membrane with less abundance in the outer membrane (Figure 4D). These data suggest that the N-terminal extended region may endow PTENα with distinct cellular localization and function and that PTENα may be involved in mitochondrial function.

Role of PTENα in Mitochondrial Respiratory Chain Function

In order to determine whether PTENα is involved in mitochondrial oxidative phosphorylation (OXPHOS), we measured the enzymatic activities of different OXPHOS complexes. We found that although the NAD/NADH ratio is reduced in *Pten* null MEFs as compared to wild-type cells, neither complexe I nor II is significantly affected (Figures S4A-S4C). Similar results were observed in cells with somatic PTENα deletion (Figures S4D-S4F). Among different OXPHOS complexes, the complex IV (cytochrome c oxidase, COX) is found to be the primary target of PTENα. Cytochrome c oxidation represents a critical feature of mitochondrial function in coupling electron transport and oxidative

phosphorylation (Coenen et al., 2001). As alternative CUG translation initiation induced by ATA can elevate endogenous PTENα (Figures 3A), we sought to determine whether induction of endogenous PTENα could enhance mitochondrial respirasome function. ATA-treated cells containing wild-type PTEN express a higher level of PTENα (Figures 5A and S5A) and consequently show an increase in COX activity (Figures 5B and S5B). These data indicate that PTENα can stimulate mitochondrial COX activity even in the presence of a substantial level of canonical PTEN.

To determine how PTENα alters mitochondrial function in the presence or absence of canonical PTEN, we transfected FLAG-tagged PTENα as well as canonical PTEN into *Pten*$^{-/-}$ MEFs for analysis of COX activity. While PTEN is expressed primarily in the cytoplasm, ectopic PTENα is found largely in the mitochondria (Figure 5C). Interestingly, the basal COX activity in *Pten*$^{-/-}$ MEFs is only 25% of that in *Pten*$^{+/+}$ cells (Figure 5D), suggesting that PTEN or PTENα is essential in mitochondrial oxidative metabolism. As deletion of PTEN simultaneously disrupts PTENα expression, it is important to clarify which of these molecules is critical for regulation of mitochondrial function. Ectopic expression of PTENα in *Pten*-null cells is able to fully rescue COX activity, whereas PTEN can also induce COX activity but to a lesser extent (Figures 5D and S5E). These data suggest that although both PTEN and PTENα are capable of maintaining COX activity, the preferential mitochondrial localization of PTENα may confer an advantage in energy metabolism.

Human MCF-7 breast cancer cells express only a trivial level of PTENα but a high level of canonical PTEN (Figure S2E), which makes MCF-7 cells a model for functional study of PTENα in the presence of canonical PTEN. We found that COX activity is increased by overexpression of PTENα in the presence of a substantial level of canonical PTEN (Figures S5C and S5D). Similarly, COX activity is induced by ectopic PTENα expression in human PC-3 prostate cancer cells null for PTEN, suggesting that PTENα can induce COX activity even in the absence of canonical PTEN. These data support the concept that PTENα plays an important role in regulation of mitochondrial function.

To further assess the relationship of PTENα with mitochondrial function, we examined PTENα localization and COX activity in various mouse tissues. Despite enrichment of PTENα in mitochondria similar to human cells, PTENα seems to be preferentially expressed in energy-consuming tissues such as skeletal and cardiac muscle (Figure 5E). More interestingly, expression levels of PTENα in different tissues correspond to levels of COX activity (Figure 5F), further highlighting the involvement of PTENα in mitochondrial respiratory chain function.

Like canonical PTEN, PTENα contains an intact phosphatase domain. To determine whether PTENα phosphatase activity is involved in mitochondrial function, we constructed a phosphatase-deficient PTENα mutant (C297S). This mutation significantly decreases PTENα-induced COX activity (Figure S5F), suggesting PTENα phosphatase function is involved in regulation of COX activity. Similar results were also observed with PTEN and its C124S mutant (Figure S5F). PTENα is preferentially localized in the inner membrane of mitochondria (Figure 4), where multi-subunit COX accumulates. Interestingly, *in vivo*

coimmunoprecipitation reveals that PTENα may physically associate with COX1 (Figure S5G). Phosphorylation of COX can regulate its activity (Huttemann et al., 2012). For example, phosphorylated COX1 at Tyr304 loses its enzymatic activity (Lee et al., 2005). These earlier studies, together with our data, imply that PTENα may regulate COX activity through maintenance of COX hypophosphorylation.

PTENα Maintains Mitochondrial Structure and Function

To evaluate the importance of PTENα, we employed transcription activator-like effector nucleases (TALEN) technology (Boch et al., 2009; Moscou and Bogdanove, 2009) to induce somatic PTENα knockout (Figure 6A). TALEN-mediated gene targeting eliminated PTENα without affecting PTEN expression (Figure 6B). Electron microscopy reveals an increased number of abnormal mitochondria with altered shape and size in PTENα$^{-/-}$ cells, manifested by much smaller mitochondria with irregular shape and dense matrix, as well as enlarged luminal vesicles (Figure 6C). We also examined mitochondrial membrane potential by staining PTENα knockout cells with JC-1 membrane-permeable dye. As shown in Figure 6D, JC-1 shows red fluorescent J-aggregates in wild type cells, indicating a hyperpolarized membrane potential. In contrast, these red J-aggregates are lost in PTENα knockout cells, and diffuse green fluorescence becomes prominent instead, indicating mitochondrial depolarization. These results suggest that PTENα depletion reduces mitochondrial membrane potential and increases permeability. Mitochondrial damage may interfere with energy metabolism, and indeed, we found a significant reduction of mitochondrial COX activity and ATP production in response to TALEN-mediated PTENα knockout (Figures 6E and 6F). These results demonstrate that PTENα is necessary for the maintenance of mitochondrial structure and function. It is of interest to note that in the presence of canonical PTEN, depletion of PTENα results in a ∼30% reduction of COX activity (Figure 6E), which is less dramatic than deletion of both *Pten* and *Pten*α in *Pten*$^{-/-}$ MEFs (>75% reduction, Figure 5D). These observations suggest that PTEN plays a role in attenuating the COX defect associated with the lack of PTENα and that these two isoforms may play a synergistic role in COX regulation.

To determine whether PTEN distribution in mitochondria may be altered by PTENα status, we compared PTEN expression and localization in the presence and absence of PTENα and found that TALEN-induced PTENα depletion results in reduced mitochondrial expression of PTEN (Figure S6A). We next employed confocal microscopy with MitoTracker as a mitochondrial marker and cotransfected *Pten*-null cells with S-tagged PTEN with or without GFP-tagged PTENα. As shown in Figure S6B, more overlapping PTEN signals were found with MitoTracker in the presence of PTENα. These data suggest that PTEN may be recruited into mitochondrial by PTENα and thus serve as one of the regulators of mitochondrial energy metabolism.

PTENα and PTEN Form a Complex and Collaborate to Increase PINK1 Protein Levels and ATP Production

Although PTENα and PTEN exhibit distinct patterns of subcellular localization (Figure 4), both can induce COX activity (Figure 5D). We therefore hypothesized that PTENα collaborates with PTEN in mitochondrial bioenergetics through formation of a PTEN-

PTENα complex. We first introduced PTENα and PTEN with different tags into 293T cells. Using S-tagged PTEN as bait, we found that FLAG-tagged PTENα exists in the S-purified protein complex (Figure 7A), indicating that PTEN can interact with PTENα. *In vivo* coimmunoprecipitation assay further confirmed the interaction between endogenous PTENα and PTEN (Figure 7B).

In order to determine how PTEN and PTENα coordinate in energy metabolism, we transfected *Pten*$^{-/-}$ MEFs with PTEN or PTENα individually and in combination (Figure S7A). The highest COX activity and ATP production were found in cells expressing both PTEN and PTENα (Figures S7B and S7C). No statistical significance was found in PTENα only versus PTENα+PTEN transfection, but this may due to the fact PTEN transfection is less efficient when cotransfected with PTENα. These data suggest that PTENα and PTEN collaborate to regulate COX activity and ATP production.

PTEN-induced kinase 1 (PINK1) is a mitochondria-targeted serine/threonine kinase that plays an important role in protection of mitochondrial function (Narendra et al., 2012; Valente et al., 2004). We found a reduced level of PINK1 expression in cells lacking PTENα (Figure 7C). Interestingly, both PTENα and PTEN can increase protein levels of PINK1 in *Pten*-null cells (Figure 7D), and PTENα seems to play a more prominent role. To translate these molecular events into readout of cellular energy, we measured ATP production in cells with ectopic PTENα, PTEN, and PINK1 individually and in combination. Each individual protein can significantly promote ATP production (Figure 7E). It is important to note that PTENα can significantly promote the ability of PTEN or PINK1 to induce ATP production, whereas addition of PTEN or PINK1 does not significantly increase the effect of PTENα. These results suggest that PTENα plays a driving role in regulating PTEN and PINK1 in energy production.

Discussion

In eukaryotes, protein translation of mRNA is typically initiated at AUG codons and the efficiency of initiation depends on the nucleotide context in which the initiator codon is embedded (Kozak, 1999). There is growing evidence including the findings in this study that shows translation initiation also occurs at non-AUG codons (Gerashchenko et al., 2010; Hann et al., 1988; Malarkannan et al., 1999; Nemeth et al., 2007), which enhances genome coding capacity and protein diversity. While CUG appears to be the most common non-AUG initiation codon (Peabody, 1989; Wegrzyn et al., 2008), the mechanism underlying CUG initiation was unknown until recently when it was shown that CUG can be decoded by a specific leucyl-tRNA to initiate alternative translation in an eIF2A-dependent pathway (Starck et al., 2012). We demonstrate that such a mechanism is responsible for the synthesis of PTENα. Bioinformatics analysis predicted a Kozak-like codon context and mRNA secondary structural features for translation initiation at CUG codons (Wegrzyn et al., 2008). In this study, we found a perfect palindromic motif centered on the PTENα CUG^{513} start codon. Because disruption of this palindrome abolishes PTENα synthesis, the palindrome sequence surrounding CUG may therefore represent a signature motif for alternative Leu-tRNA initiation (see Figure S7F). PTENα is the first non-antigenic protein that is synthesized through the Leu-tRNA initiation mechanism. The identification of PTENα

advances our understanding of protein diversity mediated by alternative translation initiation.

Recently, Hopkins et al. reported a longer form of PTEN (PTEN-Long) that is secreted into adjacent cells and antagonizes PI3K/AKT signaling (Hopkins et al., 2013). This study significantly expands the functional scope of the PTEN family from intracellular to extracellular. Although PTEN-Long was predicted to have the same translation initiation codon as PTENα based on sequence inspection, there was no peptide sequence provided or verified by mass spectrometry in the report by Hopkins et al. Based on our analysis, the CUG initiation mechanism may encode several larger forms of PTEN. It is therefore important that any longer putative PTEN isoforms be verified by mass spectrometry. As multiple forms of PTEN may exist, we consider it to be most prudent to designate PTEN isoforms as a sequential series, such as α, β or γ.

Our data demonstrate that PTENα is involved in the electron transfer reaction and ATP production likely through regulation of COX activity, the rate-limiting enzyme in the respiratory chain. Multiple mechanisms may be involved in PTENα regulation of COX activity. PTENα can promote COX activity by increasing the protein level of PINK1 as well as through physical association with COX1 and modulation of its phosphorylation status.

Based on our observations, canonical PTEN can also promote COX activity and ATP production, although to a lesser extent as compared with PTENα. Other recent reports have also suggested that PTEN may be involved in metabolic regulation (Fang et al., 2010; Garcia-Cao et al., 2012). In particular, data from super-PTEN mice suggest that additional copies of PTEN increase mitochondrial oxidative phosphorylation and ATP production (Garcia-Cao et al., 2012). As BAC-mediated transgenesis delivers the entire *Pten* locus containing the coding sequence of *Pten*α into the genome of the super-PTEN mice, the observed phenotype with this metabolic shift may result from additional copies of PTENα, or from a combination of PTEN and PTENα. PTENα shares the majority of its sequence with PTEN, and viewed in retrospect, current *Pten* knockout mouse strains are therefore essentially models of *Pten* and *Pten*α; double knockout. Thus, phenotypic deficiencies in these double knockout mice may be partially attributed to loss of *Pten*α; or its αN region. By utilizing TALEN-mediated somatic PTENα knockout, our study demonstrates the essential role of PTENα in mitochondrial bioenergetics and coordinated regulation of PINK1 with canonical PTEN.

In this study, we identify PTENα as a PTEN isoform important for mitochondrial energy metabolism. Recognition of PTENα helps understand the complexity of PTEN function and sheds light on what have previously been viewed as baffling phenomena in animal models. This study provides a model for PTENα translation through the eIF2A-mediated CUG translation initiation mechanism, and shows how the PTEN tumor suppressor family may participate in multiple distinct cellular functions. Our data demonstrate that mammalian cells can utilize the novel eIF2A/CUG/Leu-tRNA initiation mechanism to generate isoforms from what was originally thought to be a unique gene. These findings also raise the possibility that the PTEN family may have additional as yet unidentified members. Identification of

new PTEN isoforms will advance our understanding of the diversity of PTEN functions in physiological and pathological processes.

Experimental Procedures

Plasmids and Antibodies

To construct the PTENα and PTEN expression plasmids, full length PTEN cDNAs with or without an additional 5′-UTR region corresponding to CTG^{513}-TGA^{2243} or ATG^{1032}-TGA^{2243} of PTEN mRNA were amplified by PCR from HeLa cDNA and inserted with or without an N-terminal FLAG-tag into a pcDNA3.1 vector. The PTENα (CTG^{513}-TGA^{2243}) and PTEN coding sequences (ATG^{1032}-TGA^{2243}) were subcloned either into pET28a(+) for expression in bacteria or into pEGFP-N1 or pEZYMyc vector with a C-terminal GFP or Myc tag for expression in mammalian cells. Different CTG or ATG mutants were created using a site-directed mutagenesis kit (Invitrogen). The expression plasmid for eIF2A was constructed by cloning full-length eIF2A cDNA into a mammalian expression vector with an N-terminal tag.

To prepare PTENα-specific antibodies, the DNA sequence corresponding to the full-length αN region of PTENα (CTG^{513}-GAC^{1031}) was subcloned into the pET-28a vector and αN protein was purified by His affinity chromatography for antibody production in rabbits (SDIX).

Mice

A knock-in mouse strain was generated in this study by knocking a FLAG tag into the *Pten* C-terminus for identification of any potential alternative earlier translation initiations. For details, see Supplemental Experimental Procedures.

Mass Spectrometry and *de novo* Sequencing

Tissue protein lysates from $Pten^{FLAG}$ knock-in mice were subjected to FLAG pull-down followed by an additional round of immunoprecipitation using a PTENα-specific antibody. Corresponding tissues from wild-type mice ($Pten^{+/+}$) were simultaneously processed as control. Gel slices excised from $Pten^{+/+}$ and $Pten^{FLAG/+}$ samples around 70-kDa were analyzed by mass spectrometry for *in vivo* identification of Ptenα. For *in vitro* verification and *de novo* sequencing, see Supplemental Experimental Procedures.

TALEN-mediated Somatic PTENα Knockout

To specifically knockout PTENα, a TALEN binding pair was chose from PTENα CDS in the first exon between CTG^{513} and ATG^{1032}. For details, see Supplemental Experimental Procedures.

Subcellular Fractionation and Mitochondrial Subfractionation

A Millipore mitochondria/cytosol fractionation kit was used for extraction of mitochondria and nuclear/cytoplasm extraction reagents were used for separation of nuclei from cytoplasm. For subfractionation of mitochondria, see Supplemental Experimental Procedures.

Immunofluoresence and Confocal Microscopy

C-terminal GFP-tagged PTEN or PTENα were subjected to confocal microscopy for evaluation of their subcellular localization, and MitoTracker (Invitrogen) was used to indicate mitochondria.

Protease Protection Assay

A GFP tag was added to the N-terminus or C-terminus of PTEN and PTENα using pAcGFP and pEGFP plasmids for protease protection assay. The ATG^{1032} start codon of PTEN in the PTENα expression vector was mutated to ATA to avoid simultaneous PTEN expression. For details, see Supplemental Experimental Procedures.

Mitochondrial Respiratory Chain Function

Different mitochondrial respiratory chain complexes were analyzed independently with isolated mitochondria. A cytochrome c oxidase (COX) assay kit and an ATP bioluminescent assay kit (Sigma) were used for measurement of COX activity and ATP production. A JC-1 staining kit (Biotium) was used for measurement of mitochondrial membrane potential.

Statistical Analysis

Data from three independent experiments were analyzed by unpaired t test and error bars represent standard error of the mean (SEM), unless otherwise stated. The statistical significances between data sets were expressed as p values and $p < 0.05$ were considered statistical different.

Supplementary Material

Refer to Web version on PubMed Central for supplementary material.

Acknowledgments

We thank K.L. Lamb for critical reading and discussion of this work. This study was supported by NIH grants R01CA133008 and R01GM100478 to Y.Y. and W.H.S.; National Research Program of China (973 Program, 2010CB912202), National Natural Science Foundation of China (Key Project, 30930021), Beijing Natural Science Foundation (Major Project, 5100003), Peking-Tsinghua Center for Life Sciences, and Lam Chung Nin Foundation for Systems Biomedicine at Peking University.

References

Boch J, Scholze H, Schornack S, Landgraf A, Hahn S, Kay S, Lahaye T, Nickstadt A, Bonas U. Breaking the code of DNA binding specificity of TAL-type III effectors. Science. 2009; 326:1509–1512. [PubMed: 19933107]

Chen W, Lee PJ, Shion H, Ellor N, Gebler JC. Improving de novo sequencing of peptides using a charged tag and C-terminal digestion. Anal Chem. 2007; 79:1583–1590. [PubMed: 17297959]

Coenen MJ, van den Heuvel LP, Smeitink JA. Mitochondrial oxidative phosphorylation system assembly in man: recent achievements. Curr Opin Neurol. 2001; 14:777–781. [PubMed: 11723388]

Di Cristofano A, Pesce B, Cordon-Cardo C, Pandolfi PP. Pten is essential for embryonic development and tumour suppression. Nat Genet. 1998; 19:348–355. [PubMed: 9697695]

Fang M, Shen Z, Huang S, Zhao L, Chen S, Mak TW, Wang X. The ER UDPase ENTPD5 promotes protein N-glycosylation, the Warburg effect, and proliferation in the PTEN pathway. Cell. 2010; 143:711–724. [PubMed: 21074248]

Garcia-Cao I, Song MS, Hobbs RM, Laurent G, Giorgi C, de Boer VC, Anastasiou D, Ito K, Sasaki AT, Rameh L, et al. Systemic elevation of PTEN induces a tumor-suppressive metabolic state. Cell. 2012; 149:49–62. [PubMed: 22401813]

Gasser T. Update on the genetics of Parkinson's disease. Mov Disord. 2007; 22(Suppl 17):S343–350. [PubMed: 18175395]

Gerashchenko MV, Su D, Gladyshev VN. CUG start codon generates thioredoxin/glutathione reductase isoforms in mouse testes. J Biol Chem. 2010; 285:4595–4602. [PubMed: 20018845]

Hann SR, King MW, Bentley DL, Anderson CW, Eisenman RN. A non-AUG translational initiation in c-myc exon 1 generates an N-terminally distinct protein whose synthesis is disrupted in Burkitt's lymphomas. Cell. 1988; 52:185–195. [PubMed: 3277717]

Hopkins BD, Fine B, Steinbach N, Dendy M, Rapp Z, Shaw J, Pappas K, Yu JS, Hodakoski C, Mense S, et al. A Secreted PTEN Phosphatase that Enters Cells to Alter Signaling and Survival. Science. 2013

Huang ZH, Shen T, Wu J, Gage DA, Watson JT. Protein sequencing by matrix-assisted laser desorption ionization-postsource decay-mass spectrometry analysis of the N-Tris(2,4,6-trimethoxyphenyl)phosphine-acetylated tryptic digests. Anal Biochem. 1999; 268:305–317. [PubMed: 10075821]

Huttemann M, Lee I, Grossman LI, Doan JW, Sanderson TH. Phosphorylation of mammalian cytochrome c and cytochrome c oxidase in the regulation of cell destiny: respiration, apoptosis, and human disease. Adv Exp Med Biol. 2012; 748:237–264. [PubMed: 22729861]

Kozak M. Initiation of translation in prokaryotes and eukaryotes. Gene. 1999; 234:187–208. [PubMed: 10395892]

Lee I, Salomon AR, Ficarro S, Mathes I, Lottspeich F, Grossman LI, Huttemann M. cAMP-dependent tyrosine phosphorylation of subunit I inhibits cytochrome c oxidase activity. J Biol Chem. 2005; 280:6094–6100. [PubMed: 15557277]

Li J, Yen C, Liaw D, Podsypanina K, Bose S, Wang SI, Puc J, Miliaresis C, Rodgers L, McCombie R, et al. PTEN, a putative protein tyrosine phosphatase gene mutated in human brain, breast, and prostate cancer. Science. 1997; 275:1943–1947. [PubMed: 9072974]

Liaw D, Marsh DJ, Li J, Dahia PL, Wang SI, Zheng Z, Bose S, Call KM, Tsou HC, Peacocke M, et al. Germline mutations of the PTEN gene in Cowden disease, an inherited breast and thyroid cancer syndrome. Nat Genet. 1997; 16:64–67. [PubMed: 9140396]

Liu YX, Wang J, Guo J, Wu J, Lieberman HB, Yin Y. DUSP1 is controlled by p53 during the cellular response to oxidative stress. Mol Cancer Res. 2008; 6:624–633. [PubMed: 18403641]

Maehama T, Dixon JE. The tumor suppressor, PTEN/MMAC1, dephosphorylates the lipid second messenger, phosphatidylinositol 3,4,5-trisphosphate. J Biol Chem. 1998; 273:13375–13378. [PubMed: 9593664]

Malarkannan S, Horng T, Shih PP, Schwab S, Shastri N. Presentation of out-of-frame peptide/MHC class I complexes by a novel translation initiation mechanism. Immunity. 1999; 10:681–690. [PubMed: 10403643]

Moscou MJ, Bogdanove AJ. A simple cipher governs DNA recognition by TAL effectors. Science. 2009; 326:1501. [PubMed: 19933106]

Narendra D, Walker JE, Youle R. Mitochondrial quality control mediated by PINK1 and Parkin: links to parkinsonism. Cold Spring Harb Perspect Biol. 2012; 4

Nelen MR, van Staveren WC, Peeters EA, Hassel MB, Gorlin RJ, Hamm H, Lindboe CF, Fryns JP, Sijmons RH, Woods DG, et al. Germline mutations in the PTEN/MMAC1 gene in patients with Cowden disease. Hum Mol Genet. 1997; 6:1383–1387. [PubMed: 9259288]

Nemeth AL, Medveczky P, Toth J, Siklodi E, Schlett K, Patthy A, Palkovits M, Ovadi J, Tokesi N, Nemeth P, et al. Unconventional translation initiation of human trypsinogen 4 at a CUG codon with an N-terminal leucine. A possible means to regulate gene expression. FEBS J. 2007; 274:1610–1620. [PubMed: 17480209]

Peabody DS. Translation initiation at non-AUG triplets in mammalian cells. J Biol Chem. 1989; 264:5031–5035. [PubMed: 2538469]

Podsypanina K, Ellenson LH, Nemes A, Gu J, Tamura M, Yamada KM, Cordon-Cardo C, Catoretti G, Fisher PE, Parsons R. Mutation of Pten/Mmac1 in mice causes neoplasia in multiple organ systems. Proc Natl Acad Sci U S A. 1999; 96:1563–1568. [PubMed: 9990064]

Shen WH, Balajee AS, Wang J, Wu H, Eng C, Pandolfi PP, Yin Y. Essential role for nuclear PTEN in maintaining chromosomal integrity. Cell. 2007; 128:157–170. [PubMed: 17218262]

Shen WH, Wang J, Wu J, Zhurkin VB, Yin Y. Mitogen-activated protein kinase phosphatase 2: a novel transcription target of p53 in apoptosis. Cancer Res. 2006; 66:6033–6039. [PubMed: 16778175]

Song MS, Carracedo A, Salmena L, Song SJ, Egia A, Malumbres M, Pandolfi PP. Nuclear PTEN regulates the APC-CDH1 tumor-suppressive complex in a phosphatase-independent manner. Cell. 2011; 144:187–199. [PubMed: 21241890]

Stambolic V, Tsao MS, Macpherson D, Suzuki A, Chapman WB, Mak TW. High incidence of breast and endometrial neoplasia resembling human Cowden syndrome in pten+/- mice. Cancer Res. 2000; 60:3605–3611. [PubMed: 10910075]

Starck SR, Jiang V, Pavon-Eternod M, Prasad S, McCarthy B, Pan T, Shastri N. Leucine-tRNA initiates at CUG start codons for protein synthesis and presentation by MHC class I. Science. 2012; 336:1719–1723. [PubMed: 22745432]

Steck PA, Pershouse MA, Jasser SA, Yung WK, Lin H, Ligon AH, Langford LA, Baumgard ML, Hattier T, Davis T, et al. Identification of a candidate tumour suppressor gene, MMAC1, at chromosome 10q23.3 that is mutated in multiple advanced cancers. Nat Genet. 1997; 15:356–362. [PubMed: 9090379]

Stiles B, Wang Y, Stahl A, Bassilian S, Lee WP, Kim YJ, Sherwin R, Devaskar S, Lesche R, Magnuson MA, et al. Liver-specific deletion of negative regulator Pten results in fatty liver and insulin hypersensitivity [corrected]. Proc Natl Acad Sci U S A. 2004; 101:2082–2087. [PubMed: 14769918]

Stiles BL, Kuralwalla-Martinez C, Guo W, Gregorian C, Wang Y, Tian J, Magnuson MA, Wu H. Selective deletion of Pten in pancreatic beta cells leads to increased islet mass and resistance to STZ-induced diabetes. Mol Cell Biol. 2006; 26:2772–2781. [PubMed: 16537919]

Suzuki A, de la Pompa JL, Stambolic V, Elia AJ, Sasaki T, del Barco Barrantes I, Ho A, Wakeham A, Itie A, Khoo W, et al. High cancer susceptibility and embryonic lethality associated with mutation of the PTEN tumor suppressor gene in mice. Curr Biol. 1998; 8:1169–1178. [PubMed: 9799734]

Teng DH, Hu R, Lin H, Davis T, Iliev D, Frye C, Swedlund B, Hansen KL, Vinson VL, Gumpper KL, et al. MMAC1/PTEN mutations in primary tumor specimens and tumor cell lines. Cancer Res. 1997; 57:5221–5225. [PubMed: 9393738]

Valente EM, Abou-Sleiman PM, Caputo V, Muqit MM, Harvey K, Gispert S, Ali Z, Del Turco D, Bentivoglio AR, Healy DG, et al. Hereditary early-onset Parkinson's disease caused by mutations in PINK1. Science. 2004; 304:1158–1160. [PubMed: 15087508]

Wegrzyn JL, Drudge TM, Valafar F, Hook V. Bioinformatic analyses of mammalian 5′-UTR sequence properties of mRNAs predicts alternative translation initiation sites. BMC Bioinformatics. 2008; 9:232. [PubMed: 18466625]

Yin Y, Liu YX, Jin YJ, Hall EJ, Barrett JC. PAC1 phosphatase is a transcription target of p53 in signalling apoptosis and growth suppression. Nature. 2003; 422:527–531. [PubMed: 12673251]

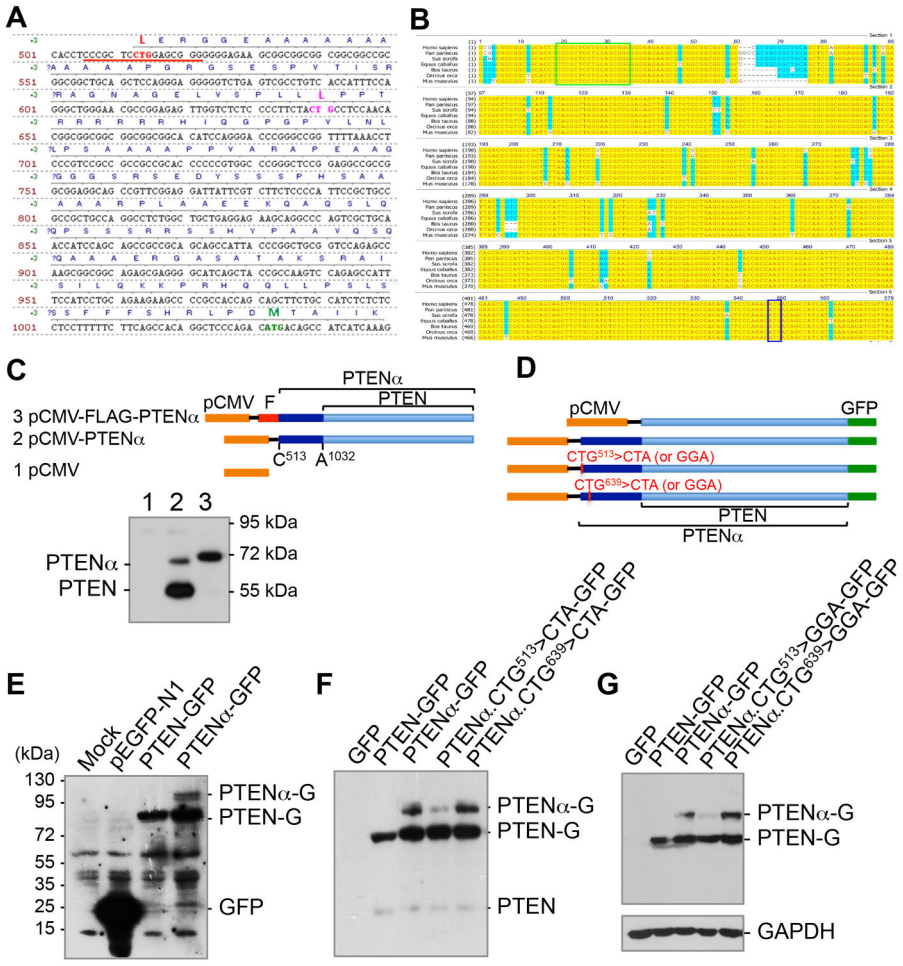

Figure 1. Identification and validation of PTENα

(A) Sequence of the 5′-UTR region of *Homo sapiens* PTEN mRNA. Two potential CUG sites (red and pink) as well as the normal ATG start site (green) are highlighted.

(B) The 5′-UTR of *PTEN* containing the 16-bp CUG-centered palindromic motif is evolutionary conserved. Phylogenetic analysis of the 5′-UTR of PTEN mRNA in bonobo (*Pan paniscus*), wild boar (*Sus scrofa*), horse (*Equus caballus*), cattle (*Bos taurus*), killer whale (*Orcinus orca*) and mouse (*Mus musculus*). The 16-bp palindromic sequence is highlighted in a green box and the ATG start codon of canonical PTEN is in a blue box.

(C) PTEN cds with a CUG^{513}-starting 5′-UTR region (PTENα) was constructed under a CMV promoter and expressed with and without a N-terminal FLAG tag. Human HEK293T cells were transfected with indicated expression plasmids, followed by Western blotting analysis using a PTEN monoclonal antibody against its C-terminal region.

(D) A different set of constructs of PTEN and PTENα with a C-terminal GFP tag, in which one of the two possible CTG sites (CTG^{513} or CTG^{639}) was mutated to CTA or GGA.

(E-G) Mutation of CTG^{513} but not CTG^{639} eliminates the expression of PTENα. C-terminal GFP-tagged PTENα expression plasmids with and without CTG^{513}>CTA or CTG^{513}>GGA mutation(s) were introduced in human HCT116 colon cancer cells, followed by detection of GFP-PTENα variants. E, The expression of GFP-tagged PTEN or PTENα was confirmed by

Western blotting using a GFP antibody. F and G, mutation of CTG^{513} but not CTG^{639} into CTA or GGA results in the disappearance of PTENα. PTENα-G and PTEN-G, PTENα or PTEN with a C-terminal GFP tag.

See also Figure S1.

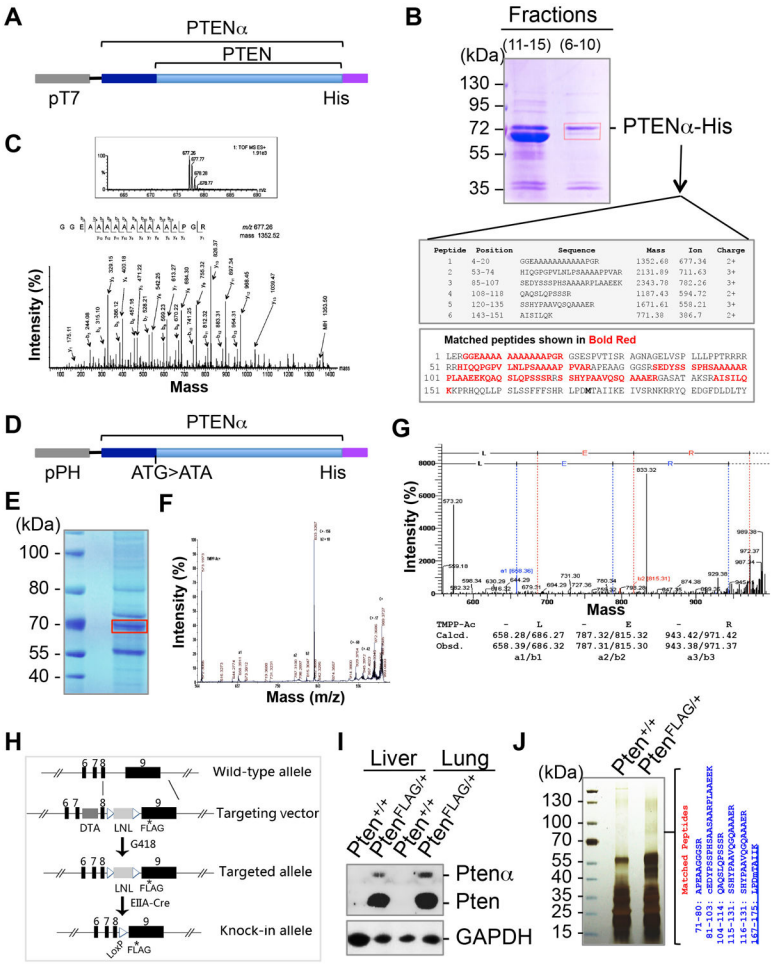

Figure 2. The translation initiation codon of PTENα is identified by MALDI-TOF mass spectrometry and terminal analysis with *de novo* sequencing

(A) A pET28a plasmid containing PTENα with a C-terminal His-tag used for *in vitro* purification and mass spectrometry sequencing.

(B) His-selected affinity purification of PTENα. Bacteria-expressed His-PTENα was purified using nickel affinity chromatography. Combined fractions containing the slow migrating PTEN band (fractions 6-10) confirmed by PTEN immunoblotting (not shown) were separated with SDS-PAGE. Mass spectrometry analysis of a purified ~70 kDa band (in red box) revealed six pieces of peptide that match the 5′-UTR region of PTEN, including a peptide near the CTG^{513}-leucine site.

(C) The MS/MS spectrum of the peptide (GGEAAAAAAAAAAPGR) that matches the N-terminus sequence of PTENα.

(D) A pFastBac1 plasmid containing PTENα with a C-terminal His-tag used for *in vitro* purification and mass spectrometry sequencing. The PTEN ATG start codon was mutated to ATA to avoid PTEN co-purification with PTENα.

(E) Purification of SF9-expressed PTENα with a C-terminal His-tag (band in red box) forMALDI-TOF-TOF MS and TMPP-Ac-OSu derivatization for *de novo* sequencing.

(F) Tandem spectrum of m/z 989.3727 in TMPP-Ac derivatized PTENα.

(G) *De novo* analysis of m/z 989.35 showing the first amino acids of PTENα, Leucine-Glutamic acid-Arginine (LER).

(H) Generation of *Pten* C-terminal FLAG knock-in mice for verification of the *Pten*α gene locus.

(I) Verification of expression of FLAG-tagged PTEN and PTENα in *Pten*-FLAG knock-in mice. Liver and lung tissues from *Pten-FLAG* knock-in mice or control wild-type mice were lysed for immunoblotting with anti-FLAG antibody.

(J) Protein lysates of *Pten-FLAG* knock-in liver tissues or control tissues were subjected to sequential immunoprecipitation with anti-FLAG M2 agarose and a PTENα-specific antibody. The bound proteins were separated with SDS-PAGE and gel slices at around 70-kDa were analyzed by mass spectrometry. Four peptides were identified in *Pten*-FLAG knock-in tissues that match the N-terminally extended region of PTENα, αN.

See also Figure S2.

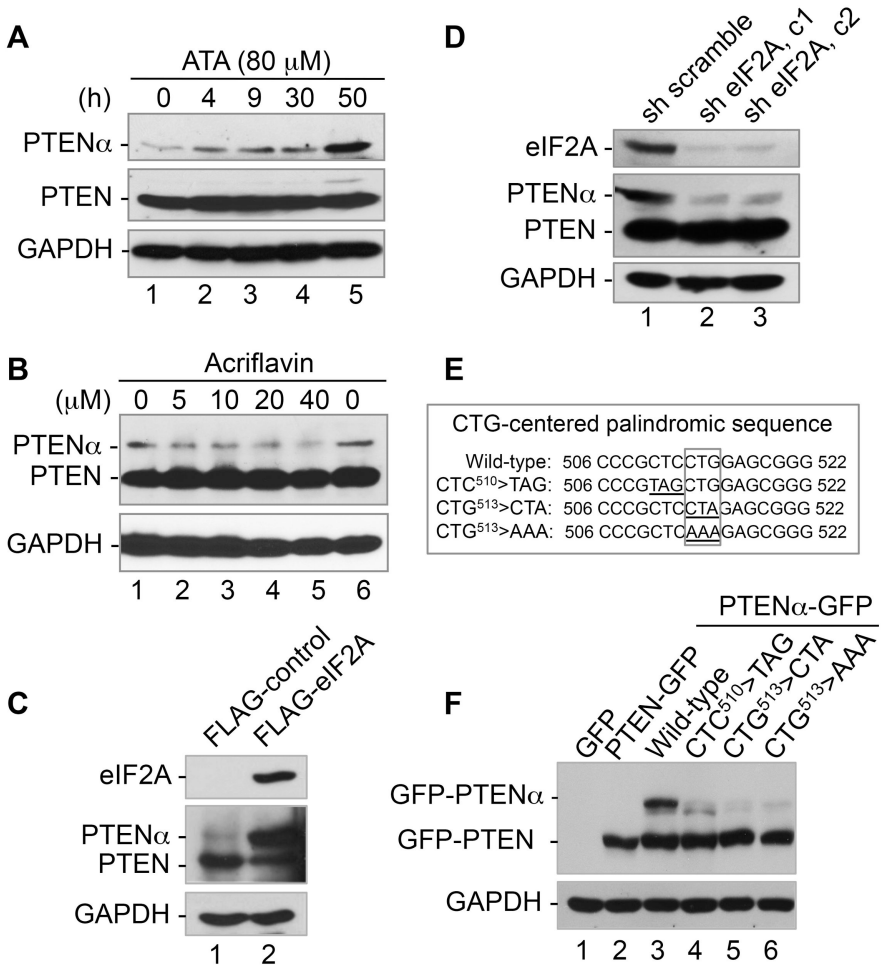

Figure 3. PTENα is synthesized through an eIF2A-mediated CUG initiation mechanism and a palindrome sequence is essential for PTENα expression

(A) Induction of PTENα by aurin tricarboxylic acid (ATA) in a time-dependent manner. HeLa cells were treated with ATA (80 mM) for various periods of time and the expression of PTENα as well as PTEN was examined by Western blot.

(B) Dose-dependent inhibition of PTENα expression by acriflavin. HeLa cells were treated with different doses of acriflavin for 4 h prior to immunoblotting for evaluation of PTENα expression. Expression levels of PTEN and GAPDH were included as controls.

(C) eIF2A alters the ratio of PTENα versus PTEN by up-regulating PTENα and down-regulating PTEN. FLAG-tagged eIF2A was overexpressed in HEK293T cells prior to Western evaluation of PTENα and PTEN. eIF2A expression was verified by probing the same blot with anti-FLAG antibody. GAPDH was used as a loading control.

(D) Reduction of PTENα in response to knockdown of eIF2A. HeLa cells were infected with lentivirus expressing shRNA of eIF2A or scramble shRNA. Cell lysates were analyzed by Western blotting with antibodies against eIF2A, PTEN (m) and GAPDH.

(E) CTG^{513}-centered palindromic sequence and mutagenesis disruption of the palindrome.

(F) Abolition of PTENα by palindrome disruption. Mutations were made at CTC^{510}, thetriplet immediately before the CTG^{513} start codon, or at CUG^{513} itself as indicated prior to Western analysis of PTENα expression.

See also Figure S3.

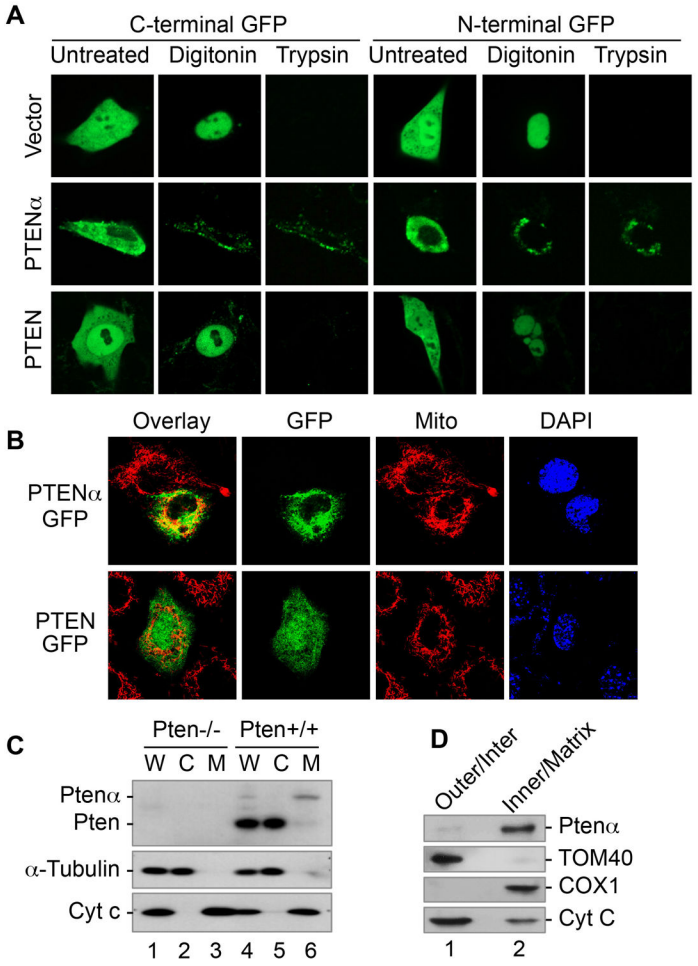

Figure 4. PTENα is localized predominantly in cytoplasm and mitochondria

(A) *Pten*$^{-/-}$ MEFs transfected with N-terminal or C-terminal GFP-tagged PTEN or PTENα were subjected to protease protection assay, confirming the difference in subcellular distribution patters of PTENα and PTEN.

(B) Subcellular localization of C-terminal GFP-tagged PTENα (with an ATG>ATA mutation) and PTEN shown by confocal fluorescence microscopy. MitoTracker was used to indicate mitochondria. Overlay, merged images of GFP and MitoTracker.

(C) Cell fractionation was performed to isolate mitochondria in *Pten*$^{+/+}$ and *Pten*$^{-/-}$ MEFs prior to immunoblotting analysis of PTENα and PTEN expression. W, whole cell lysate; M, mitochondria; C, cytoplasm. Cytochrome c and a-tubulin were used as mitochondrial and cytoplasmic markers.

(D) Mitochondria isolated from mouse brain cortex were subjected to sub fractionation of mitochondria prior to evaluation of PTENα by immunoblotting. Tom40 and Cox1 were used as markers for the mitochondrial outer membrane and inner membrane respectively. Cytochrome C is a dynamic component of mitochondria and can be found in both the inner membrane and intermembrane space.

See also Figures S4-S7.

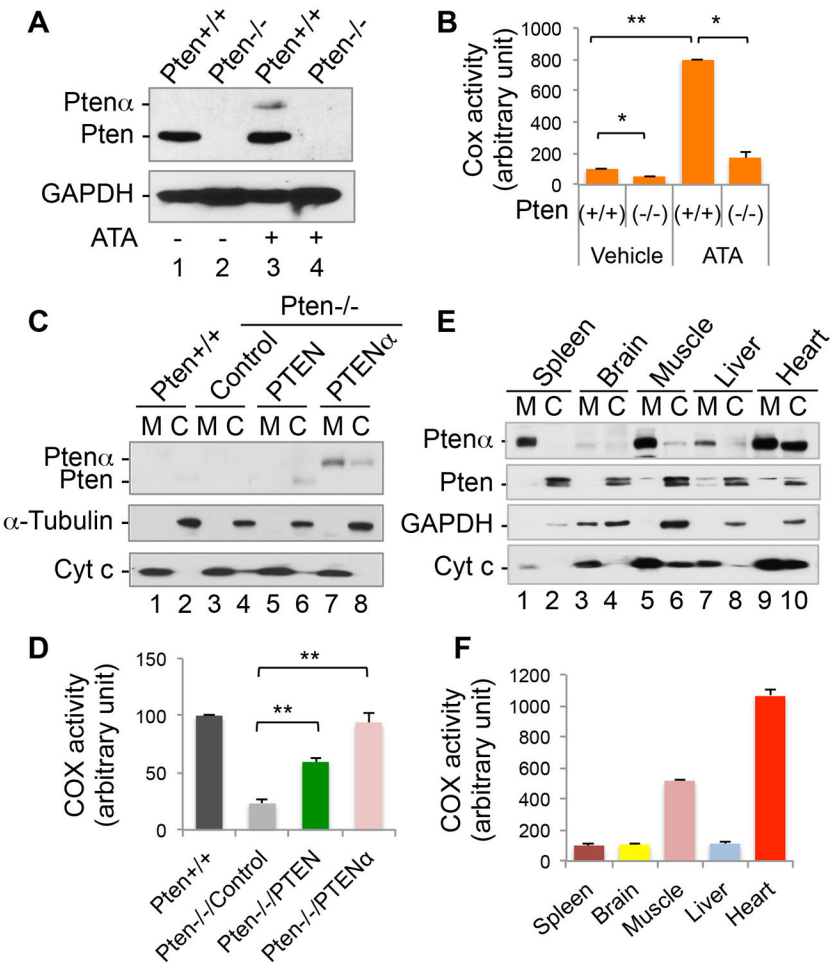

Figure 5. PTENα regulates cytochrome c oxidase activity

(A) *Pten*$^{+/+}$ and *Pten* $^{-/-}$ MEFs were treated with ATA (100mM, 24 h) and examined for expression levels of PTEN and PTENα.

(B) Mitochondrial fractions were extracted from *Pten*$^{+/+}$ and *Pten*$^{-/-}$ MEFs treated with ATA as in (A) for analysis of cytochrome c oxidatase (COX) activity. Data are presented as mean ±SEM of three independent experiments and analyzed with the paired t-test. *, p <0.05; **, p <0.01.

(C) *Pten*$^{+/+}$ and *Pten*$^{-/-}$ MEFs with and without ectopic expression of FLAG-tagged PTEN or PTENα were subjected to a cell fractionation procedure for isolation of mitochondria, followed by immunoblot analysis of PTEN/PTENα expression. Cytochrome c and α-tubulin were used as mitochondrial and cytoplasmic markers. M, mitochondria; C, cytoplasm.

(D) Mitochondria from *Pten*$^{+/+}$ MEFs as well as from *Pten*$^{-/-}$ MEFs containing ectopic PTEN or PTENα were analyzed for COX activity. Data are presented as mean±SEM of three independent experiments and analyzed by paired t-test. **, p <0.01.

(E) Various mouse tissues were subjected to mitochondria/cytoplasm fractionation, followed by Western analysis of PTENα expression. PTEN expression is also shown for comparison. GAPDH and cytochrome c were used as cytoplasmic and mitochondrial markers.

(F) Mitochondria were extracted from various mouse tissues as indicated for analysis of COX activity.

See also Figures S4-S7.

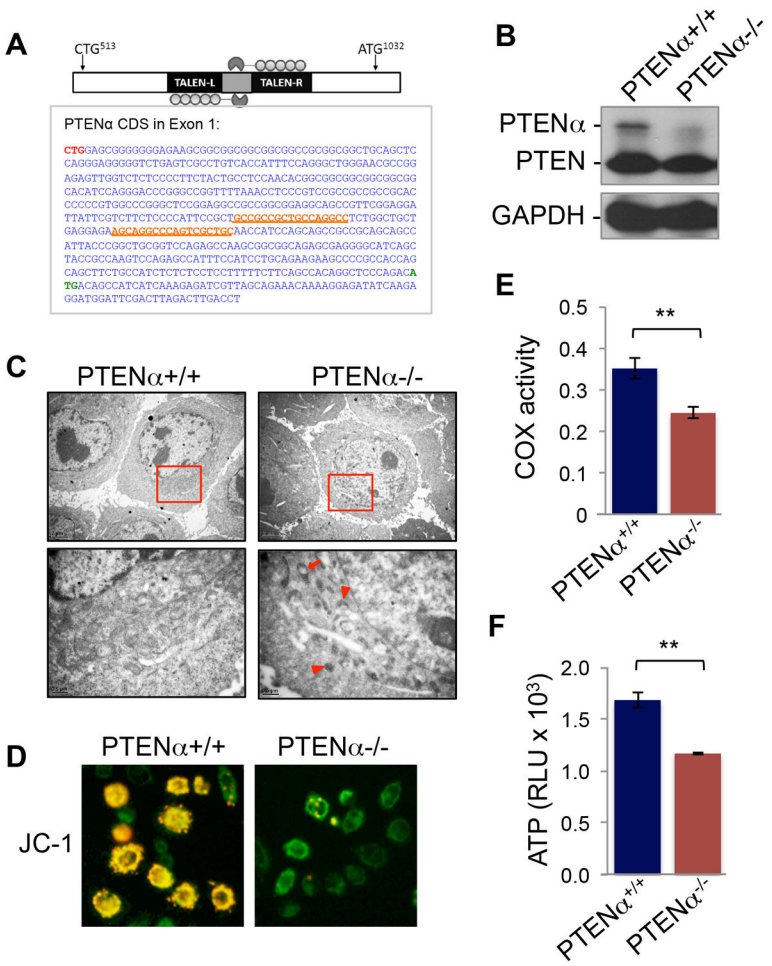

Figure 6. Somatic knockout of PTENα impairs mitochondrial structure and function

(A) Somatic knockout of PTENα with the TALEN technique. Upper panel, schematic strategy of PTENα TALEN knockout. Lower panel, sequence of PTENα CDS in exon 1. TALEN targeted left and right arms are underlined and highlighted in orange. CTG^{513} and ATG^{1032} are highlighted in red and green respectively.

(B) Western blot confirming elimination of PTENα.

(C) Marked mitochondrial morphological alterations in $PTEN\alpha^{-/-}$ HeLa cells shown by electron microscopy. Arrowheads indicate smaller condensed mitochondria. The arrow points to a mitochondrion with expanded vesicles.

(D) JC-1 staining showing loss of red-J-aggregate fluorescence in $PTEN\alpha^{-/-}$ cells (right) as compared with $PTEN\alpha^{+/+}$ cells (left).

(E) Impaired COX activity in $PTEN\alpha^{-/-}$ cells. Mitochondria were extracted from $PTEN\alpha^{+/+}$ and $PTEN\alpha^{-/-}$ cells for analysis of COX activity.

(F) PTENα knockout reduces ATP production. Data are presented as mean±SD of three replicates and analyzed by paired t-test. **, p <0.01.

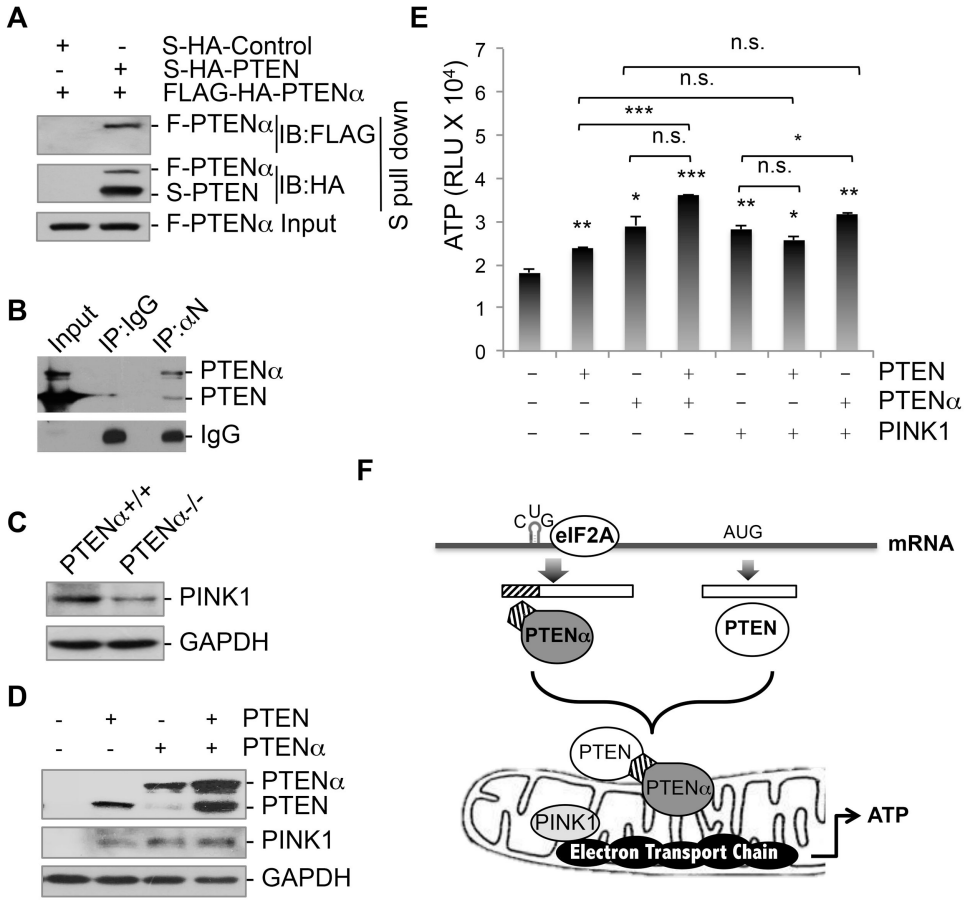

Figure 7. PTENα and PTEN form a complex and collaborate in energy metabolism

(A) S-HA-tagged PTEN and FLAG-HA-tagged PTENα were transfected into 293T cells prior to S protein pull-down (S-PD). FLAG or HA immunoblotting was performed to detect PTEN-associated PTENα.

(B) *In vivo* binding of PTENα with PTEN. Endogenous PTENα was immunoprecipited using anti-αN antibody from mouse brain tissues for immunoblotting of PTEN.

(C) Evaluation of PINK1 expression in PTENα depleted cells by Western blotting.

(D) PINK1 expression was assessed in *Pten*$^{-/-}$ MEFs transfected with PTEN, PTENα, or PTEN+PTENα.

(E) *Pten*$^{-/-}$ MEFs transfected individually or in different combinations with PTEN, PTENα and PINK1, followed by analysis of ATP production. Data are presented as mean±SD. Labeling for statistical significance above each column indicates a comparison with the control column. n.s. not significant, $p>0.05$; *, $p<0.05$; **, $p<0.01$; ***, $p<0.001$.

(F) A graphic model of PTENα translation and its function in mitochrondrial energy metabolism. PTENα is synthesized through an eIF2A- and palindrome-dependent CUG initiation mechanism. PTENα forms a complex with canonical PTEN and these molecules collaborate in mitochondrial bioenergetics through regulation of cytochrome c oxidase activity and ATP production.

See also Figures S6 and S7.